
SurCo: Learning Linear SURrogates for COmbinatorial Nonlinear Optimization Problems

Anonymous Author(s)

Affiliation

Address

email

Abstract

1 Optimization problems with nonlinear cost functions and combinatorial constraints
2 appear in many real-world applications but remain challenging to solve efficiently
3 compared to their linear counterparts. To bridge this gap, we propose **SurCo**
4 that learns linear Surrogate costs which can be used in existing Combinatorial
5 solvers to output good solutions to the original nonlinear combinatorial optimization
6 problem. The surrogate costs are learned end-to-end with nonlinear loss by
7 differentiating through the linear surrogate solver, combining the flexibility of
8 gradient-based methods with the structure of linear combinatorial optimization. We
9 propose three SurCo variants: SurCo – zero for individual nonlinear problems,
10 SurCo – prior for problem distributions, and SurCo – hybrid to combine
11 both distribution and problem-specific information. We give theoretical intuition
12 motivating SurCo, and evaluate it empirically. Experiments show that SurCo
13 finds better solutions faster than state-of-the-art and domain expert approaches
14 in real-world optimization problems such as embedding table sharding, inverse
15 photonic design, and nonlinear route planning.

16 1 Introduction

17 Combinatorial optimization problems with linear objective functions such as mixed integer linear pro-
18 gramming (MILP) (Wolsey, 2007), and occasionally linear programming (LP) (Chvatal et al., 1983),
19 have been extensively studied in operations research (OR). The resulting high-performance solvers
20 like Gurobi (Gurobi Optimization, LLC, 2022) can solve industrial-scale optimization problems with
21 tens of thousands of variables in a few minutes.

22 However, even with perfect solvers, one issue remains: the cost functions $f(\mathbf{x})$ in many practical
23 problems are *nonlinear*, and the highly-optimized solvers mainly handle linear or convex formulations
24 while real-world problems have less constrained objectives. For example, in embedding table
25 sharding (Zha et al., 2022a) one needs to distribute embedding tables to multiple GPUs for the
26 deployment of recommendation systems. Due to the batching behaviors within a single GPU and
27 communication cost among different GPUs, the overall latency (cost function) in this application
28 depends on interactions of multiple tables and thus can be highly nonlinear (Zha et al., 2022a).

29 To obtain useful solutions to real-world problems, one may choose to directly optimize the nonlinear
30 cost, which can be the black-box output of a simulator (Gosavi et al., 2015; Ye et al., 2019), or the
31 output of a cost estimator learned by machine learning techniques (e.g., deep models) from offline
32 data (Steiner et al., 2021; Koziel et al., 2021; Wang et al., 2021b; Cozad et al., 2014). However, many
33 of these direct optimization approaches either rely on human-defined heuristics (e.g., greedy (Korte
34 & Hausmann, 1978; Reingold & Tarjan, 1981; Wolsey, 1982), local improvement (Voß et al., 2012;
35 Li et al., 2021)), or resort to general nonlinear optimization techniques like gradient descent (Ruder,
36 2016), reinforcement learning (Mazyavkina et al., 2021), or evolutionary algorithms (Simon, 2013).

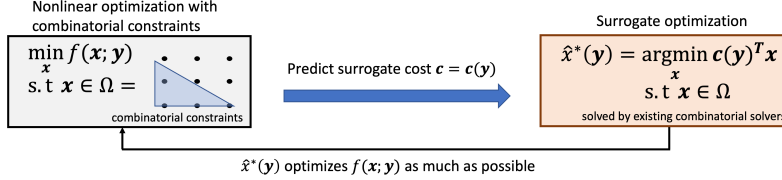


Figure 1: Overview of our proposed framework `SurCo`.

37 While these approaches can work in certain settings, they may lead to a slow optimization process, in
 38 particular when the cost function is expensive to evaluate, and they often ignore the combinatorial
 39 nature of most real-world applications.

40 In this work, we propose a systematic framework **SurCo** that leverages existing efficient combinatorial
 41 solvers to find solutions to nonlinear combinatorial optimization problems arising in
 42 real-world scenarios. When only one nonlinear *differentiable* cost $f(x)$ needs to be minimized, we
 43 propose `SurCo-zero` that optimizes a *linear surrogate* cost \hat{c} so that the *surrogate optimizer* (SO)
 44 $\min_{x \in \Omega} \hat{c}^\top x$ outputs a solution that is expected to be optimal w.r.t. the *original* nonlinear cost $f(x)$.
 45 Due to its linear nature, SO can be solved efficiently with existing solvers, and the surrogate cost
 46 \hat{c} can be optimized in an end-to-end manner by back-propagating *through* the solver via methods
 47 proposed in previous work (Pogančić et al., 2019; Niepert et al., 2021; Berthet et al., 2020).

48 Thus, `SurCo` is a general-purpose method for solving combinatorial nonlinear optimization. Off-
 49 the-shelf nonlinear optimizers are often not directly applicable to these problem domains and often
 50 require domain-specific solution methodologies to give high-quality solutions in a reasonable amount
 51 of time, and solution prediction methods fail to give combinatorially feasible solutions without
 52 problem-specific intervention. Here, learning a linear surrogate problem ensures that the surrogate
 53 solver is practically efficient, yields gradient information for offline training, and generates solutions
 54 that are combinatorially feasible.

55 When solving a family of nonlinear differentiable functions $f(x; y)$ parameterized by instance
 56 description y , the surrogate *coefficients* $\hat{c}(y; \theta)$ are learned on a set of optimization instances (called
 57 the training set $\{y_i\}$), by optimizing the parameters θ . For an unseen held-out instance y' , we
 58 propose `SurCo-prior` that directly optimizes linear SO: $\hat{x}^*(y') := \arg \min_{x \in \Omega(y')} \hat{c}^\top(y'; \theta)x$ to
 59 get the solution, avoiding optimizing the cost $f(x; y')$ from scratch. Based on the solution predicted
 60 by `SurCo-prior`, we also propose `SurCo-hybrid` that fine-tunes the surrogate costs \hat{c} with
 61 `SurCo-zero` to leverage both domain knowledge synthesized offline and information about the
 62 specific instance. We provide a comprehensive description of `SurCo` in Section 3.

63 We evaluate `SurCo` in three settings: embedding table sharding (Zha et al., 2022a), photonic inverse
 64 design (Schubert et al., 2022), and nonlinear route planning Fan et al. (2005). In the on-the-fly setting,
 65 `SurCo-zero` achieves higher quality solutions in comparable or less runtime, thanks to the help of
 66 an efficient combinatorial solver. In `SurCo-prior`, our method obtains better solutions in held-out
 67 problems compared to other methods that require training (e.g., reinforcement learning).

68 We compare `SurCo` at a high level with related work integrating learning and optimization at the end
 69 of our paper. We additionally present theoretical intuition that helps motivate why training a model to
 70 predict surrogate linear coefficients may exhibit better sample complexity than previous approaches
 71 that directly predict the optimal solution (Li et al., 2018; Ban & Rudin, 2019).

72 2 Problem Specification

73 Our goal is to solve the following nonlinear optimization problem describe by y :

$$\min_x f(x; y) \quad \text{s.t.} \quad x \in \Omega(y) \quad (1)$$

74 where $x \in \mathbb{R}^n$ are the n variables to be optimized, $f(x; y)$ is the nonlinear differentiable cost
 75 function to be minimized, $\Omega(y)$ is the feasible region, typically specified by linear (in)equalities and
 76 integer constraints, and $y \in Y$ are the problem instance parameters drawn from a distribution \mathcal{D} over
 77 Y . For example, in the traveling salesman problem, y can be the distance matrix among cities.

78 **Differentiable cost function.** The nonlinear cost function $f(x; y)$ can either be given analytically, or
 79 the result of a simulator made differentiable via finite differencing (e.g., JAX (Bradbury et al., 2018)).

Methods	Applicable to nonlinear objective	Objective can be free form	Training Set	Generalize to new instances	Combinatorial constraints
Gradient Descent	Yes	Yes	N/A	No	No
Evolutionary Algorithm	Yes	Yes	N/A	No	No
Nonlinear combinatorial solvers	Yes	No	N/A	No	Yes
Learning direct mapping	Yes	Yes	$\{\mathbf{y}_i, \mathbf{x}_i^*\}$	Yes	No
Predict-then-optimize	Limited	No	$\{\mathbf{y}_i, \mathbf{x}_i^*\}$	Yes	Yes
SurCo (proposed)	Yes	Yes	$\{\mathbf{y}_i\}$	Yes	Yes

Table 1: Conceptual comparison of optimizers (both traditional and ML-guided). Our approach (SurCo) can handle nonlinear objective without a predefined analytical form, does not require pre-computed optimal solutions in its training set, can handle combinatorial constraints (via commercial solvers it incorporates), and can generalize to unseen instances.

80 If the cost function $f(\mathbf{x}; \mathbf{y})$ is not differentiable as in one of our experimental settings, we can use
81 a cost model that is learned from an offline dataset, often generated via sampling multiple feasible
82 solutions within $\Omega(\mathbf{y})$, and recording their costs. In this work, we assume the following of $f(\mathbf{x}; \mathbf{y})$:

83 **Assumption 2.1** (Differentiable cost function). During optimization, the cost function $f(\mathbf{x}; \mathbf{y})$ and
84 its partial derivative $\partial f / \partial \mathbf{x}$ are accessible.

85 Learning a good nonlinear cost model f is non-trivial for practical applications (e.g., Al-
86 phaFold (Jumper et al., 2021), Density Functional Theory (Nagai et al., 2020), cost model for
87 embedding tables (Zha et al., 2022a)) and is beyond the scope of this work.

88 **Evaluation Metric.** We mainly focus on two aspects: the solution quality evaluated by $f(\hat{\mathbf{x}}; \mathbf{y})$,
89 and the number of queries of f during optimization to achieve the solution $\hat{\mathbf{x}}$. For both, smaller
90 measurements are favorable, i.e., fewer query of f to get solutions closer to global optimum.

91 When $f(\mathbf{x}; \mathbf{y})$ is linear w.r.t \mathbf{x} , and the feasible region $\Omega(\mathbf{y})$ can be encoded using mixed integer
92 programs, the problem can be solved using existing scalable optimization solvers. When $f(\mathbf{x}; \mathbf{y})$ is
93 nonlinear, we propose SurCo that learns a surrogate linear objective function, which allow us to
94 leverage these existing scalable optimization solvers, and results in a solution that has high quality
95 with respect to the original hard-to-encode objective function $f(\mathbf{x}; \mathbf{y})$.

96 3 SurCo: Learning Linear Surrogates

97 **SurCo-zero: on-the-fly optimization.** We start from the simplest case where we focus on a single
98 instance with $f(\mathbf{x}) = f(\mathbf{x}; \mathbf{y})$ and $\Omega = \Omega(\mathbf{y})$. SurCo-zero optimizes the following objective:

$$(SurCo-zero): \min_{\mathbf{c}} \mathcal{L}_{zero}(\mathbf{c}) := f(\mathbf{g}_{\Omega}(\mathbf{c})) \quad (2)$$

99 where the surrogate optimizer $\mathbf{g}_{\Omega} : \mathbb{R}^n \mapsto \mathbb{R}^n$ is the output of certain combinatorial solvers with
100 linear cost weight $\mathbf{c} \in \mathbb{R}^n$ and feasible region $\Omega \subseteq \mathbb{R}^n$. For example, \mathbf{g}_{Ω} can be the following:

$$\mathbf{g}_{\Omega}(\mathbf{c}) := \arg \min_{\mathbf{x}} \mathbf{c}^{\top} \mathbf{x} \quad \text{s.t.} \quad \mathbf{x} \in \Omega := \{A\mathbf{x} \leq \mathbf{b}, \mathbf{x} \in \mathbb{Z}^n\} \quad (3)$$

101 which is the output of a MILP solver. Thanks to previous works (Ferber et al., 2020; Pogančić et al.,
102 2019), we can efficiently compute the partial derivative $\partial \mathbf{g}_{\Omega}(\mathbf{c}) / \partial \mathbf{c}$. Intuitively, this means that
103 $\mathbf{g}_{\Omega}(\mathbf{c})$ can be *backpropagated* through. Since f is also differentiable with respect to the solution it is
104 evaluating, we thus can optimize Eqn. 2 in an end-to-end manner using any gradient-based optimizer:

$$\mathbf{c}(t+1) = \mathbf{c}(t) - \alpha \frac{\partial \mathbf{g}_{\Omega}}{\partial \mathbf{c}} \frac{\partial f}{\partial \mathbf{x}}, \quad (4)$$

105 where α is the learning rate. The procedure starts from a randomly initialized $\mathbf{c}(0)$ and converges at a
106 local optimal solution of \mathbf{c} . While Eqn. 2 is still nonlinear optimization and there is no guarantee
107 about the quality of the final solution \mathbf{c} , we argue that optimizing Eqn. 2 is better than optimizing
108 the original nonlinear cost $\min_{\mathbf{x} \in \Omega} f(\mathbf{x})$. Furthermore, while we cannot guarantee optimality, we
109 guarantee feasibility by leveraging a linear combinatorial solver.

110 Intuitively, instead of optimizing directly over the solution space \mathbf{x} , we optimize over the space of
111 surrogate costs \mathbf{c} , and delegate the combinatorial feasibility requirements of the nonlinear problem to
112 SoTA combinatorial solvers. Compared to naive approaches that directly optimize $f(\mathbf{x})$ via
113 general optimization techniques, our method readily handles complex constraints of the feasible

114 regions, and thus makes the optimization procedure easier. Furthermore, it also helps escape from
 115 local minima, thanks to the embedded search component of existing combinatorial solvers (e.g.,
 116 branch-and-bound (Land & Doig, 2010) in MILP solvers). As we see in the experiments, this is
 117 particularly important when the problem becomes large-scale with more local optima. This approach
 118 works well when we are optimizing individual instances and may not have access to offline training
 119 data or the training time is cost-prohibitive.

120 **Limitation.** Note that due to linear surrogate, our approach will always return a vertex in the feasible
 121 region, while the solution to the original nonlinear objective may be in the interior. We leave this
 122 limitation for future work. In many real-world settings, such as in the three domains we tested, the
 123 solutions are indeed on the vertices of feasible regions.

124 **SurCo-prior: offline surrogate training.** We now consider a more general case where we have
 125 N optimization instances, each parameterized by an instance description \mathbf{y}_i , $i = 1 \dots N$, and we
 126 want to find their solutions to a *collection* of nonlinear loss functions $f(\mathbf{x}; \mathbf{y}_i)$ simultaneously. Here
 127 we write $\mathcal{D}_{\text{train}} := \{\mathbf{y}_i\}_{i=1}^N$ as the training set. A naive approach is just to apply SurCo-zero
 128 N times, which leads to N independent surrogate costs $\{c_i\}_{i=1}^N$. However, this approach does not
 129 consider two important characteristics. *First*, it fails to leverage possible relationship between the
 130 instance descriptor \mathbf{y}_i and its associated surrogate cost c_i , since every surrogate cost is independently
 131 estimated. *Second*, it fails to learn any useful knowledge from the N instances after optimization. As
 132 a result, for an unseen instance, the entire optimization process needs to be conducted again, which is
 133 slow. This motivates us to add a surrogate cost *model* $\hat{c}(\mathbf{y}; \boldsymbol{\theta})$ into the optimization as a regularizer:

$$\text{(SurCo-prior-}\lambda\text{)}: \min_{\boldsymbol{\theta}, \{c_i\}} \mathcal{L}_{\text{prior}}(\boldsymbol{\theta}, \{c_i\}; \lambda) := \sum_{i=1}^N f(g_{\Omega(\mathbf{y}_i)}(c_i; \mathbf{y}_i) + \lambda \|c_i - \hat{c}(\mathbf{y}_i; \boldsymbol{\theta})\|_2)$$

134 The regressor model $\hat{c}(\mathbf{y}; \boldsymbol{\theta})$ directly predicts the surrogate cost from the instance description. The
 135 form of the regressor can be a neural network, in which $\boldsymbol{\theta}$ is its parameters. Note that when $\lambda = 0$, it
 136 reduces to N independent optimizations, while when $\lambda > 0$, the surrogate costs $\{c_i\}$ interact with
 137 each other. With the regressor, we distill knowledge gained from the optimization procedure into $\boldsymbol{\theta}$,
 138 which can be used for an unseen instance \mathbf{y}' . Indeed, we use the learned regressor model to predict
 139 the surrogate cost $c' = \hat{c}(\mathbf{y}'; \boldsymbol{\theta})$, and directly solve the *surrogate optimization* (SO):

$$\hat{\mathbf{x}}^*(\mathbf{y}') = \arg \min_{\mathbf{x} \in \Omega(\mathbf{y}')} \hat{c}^\top(\mathbf{y}'; \boldsymbol{\theta}) \mathbf{x} \quad (5)$$

140 A special case is when $\lambda \rightarrow +\infty$, we learn the network parameters $\boldsymbol{\theta}$ instead of surrogate costs:

$$\text{(SurCo-prior)}: \min_{\boldsymbol{\theta}} \mathcal{L}_{\text{prior}}(\boldsymbol{\theta}) := \sum_{i=1}^N f(g_{\Omega(\mathbf{y}_i)}(\hat{c}(\mathbf{y}_i; \boldsymbol{\theta})); \mathbf{y}_i)$$

141 This approach is useful when the goal is to find high-quality solutions for unseen instances of a
 142 problem distribution when the upfront cost of offline training is acceptable but the cost of optimizing
 143 on-the-fly is prohibitive. Here, we require access to a distribution of training optimization problems,
 144 but at test time only require the feasible region and not the nonlinear objective. Different from
 145 predict-then-optimize Elmachtoub & Grigas (2022a); Ferber et al. (2020) or ML optimizers Ban &
 146 Rudin (2019), we do not require the optimal solution $\{\mathbf{x}_i^*\}_{i=1}^N$ as part of the training set.

147 **SurCo-hybrid: fine-tuning a predicted surrogate.** Naturally, we consider SurCo-hybrid, a
 148 hybrid approach which initializes the coefficients of SurCo-zero with the coefficients predicted
 149 from SurCo-prior which was trained on offline data. This allows SurCo-hybrid to start out
 150 optimization from an initial prediction that has good performance for the distribution at large but
 151 which is then fine-tuned for the specific instance. Formally, we initialize $\mathbf{c}(0) = \hat{c}(\mathbf{y}_i; \boldsymbol{\theta})$ and then
 152 continue optimizing \mathbf{c} based on the update from SurCo-zero. This approach is geared towards
 153 optimizing the nonlinear objective using a high-quality initial prediction that is based on the problem
 154 distribution and then fine-tuning the objective coefficients based on the specific problem instance
 155 at test time. Here, high performance comes at the runtime cost of both having to train offline on a
 156 problem distribution as well as performing fine-tuning steps on-the-fly. However, this additional
 157 cost is often worthwhile when the main goal is to find the best possible solutions by leveraging
 158 synthesized domain knowledge in combination with individual problem instances as arises in chip
 159 design (Mirhoseini et al., 2021) and compiler optimization (Zhou et al., 2020).

160 4 Surrogate Costs vs Solution Prediction, A Theoretical Analysis

161 One of the key ingredient of our proposed methods (SurCo-prior and SurCo-hybrid) is to
 162 learn a model to predict surrogate cost c from instance description \mathbf{y} , which is in contrast with
 163 previous solution regression approaches that directly learn a mapping from problem description \mathbf{y} to
 164 the solution $\mathbf{x}^*(\mathbf{y})$ (Ban & Rudin, 2019). A natural question arise: which one is better?

165 In this section, we give theoretical intuition to compare the two approaches using a simple 1-nearest-
 166 neighbor (1-NN) solution regressor (Fix, 1985). We first relate the number of samples needed to learn
 167 any mapping to its *Lipschitz constant* L , and then show that for the direct mapping $\mathbf{y} \mapsto \mathbf{x}^*(\mathbf{y})$, L
 168 can be very large. Therefore, there exist fundamental difficulties to learn such a mapping. When this
 169 happens, we can still find surrogate cost mapping $\mathbf{y} \mapsto c^*(\mathbf{y})$ with finite L that leads to the optimal
 170 solution $\mathbf{x}^*(\mathbf{y})$ of the original nonlinear problems.

171 **Lipschitz constant and sample complexity.** Formally, consider fitting any mapping $\phi : \mathbb{R}^d \supseteq$
 172 $Y \mapsto \mathbb{R}^m$ with a dataset $\mathcal{C} := \{\mathbf{y}_i, \phi_i\}$. Here Y is a compact region with finite volume $\text{vol}(Y)$. The
 173 Lipschitz constant L is the smallest number so that $\|\phi(\mathbf{y}_1) - \phi(\mathbf{y}_2)\|_2 \leq L\|\mathbf{y}_1 - \mathbf{y}_2\|_2$ holds for any
 174 $\mathbf{y}_1, \mathbf{y}_2 \in Y$. The following theorem shows that if the dataset covers the space Y , we could achieve
 175 high accuracy prediction: $\|\phi(\mathbf{y}) - \hat{\phi}(\mathbf{y})\|_2 \leq \epsilon$ for any $\mathbf{y} \in Y$.

176 **Definition 4.1** (δ -cover). A dataset $\mathcal{C} := \{(\mathbf{y}_i, \phi_i)\}_{i=1}^N$ δ -covers the space Y , if for any $\mathbf{y} \in Y$, there
 177 exists at least one \mathbf{y}_i so that $\|\mathbf{y} - \mathbf{y}_i\|_2 \leq \delta$.

178 **Lemma 4.2** (Sufficient condition of prediction with ϵ -accuracy). *If the dataset \mathcal{C} can (ϵ/L) -cover Y ,*
 179 *then for any $\mathbf{y} \in Y$, a 1-nearest-neighbor regressor $\hat{\phi}$ leads to $\|\hat{\phi}(\mathbf{y}) - \phi(\mathbf{y})\|_2 \leq \epsilon$.*

180 **Lemma 4.3** (Lower bound of sample complexity for ϵ/L -cover). *To achieve ϵ/L -cover of Y , the size*
 181 *of the dataset set $N \geq N_0(\epsilon) := \frac{\text{vol}(Y)}{\text{vol}_0} \left(\frac{L}{\epsilon}\right)^d$, where vol_0 is the volume of unit ball in d -dimension.*

182 Please find all proofs in the Appendix. While we do not rule out a more advanced regressor than
 183 1-nearest-neighbor that could lead to better sample complexity, the lemmas demonstrate that the
 184 Lipschitz constant L plays an important role in sample complexity.

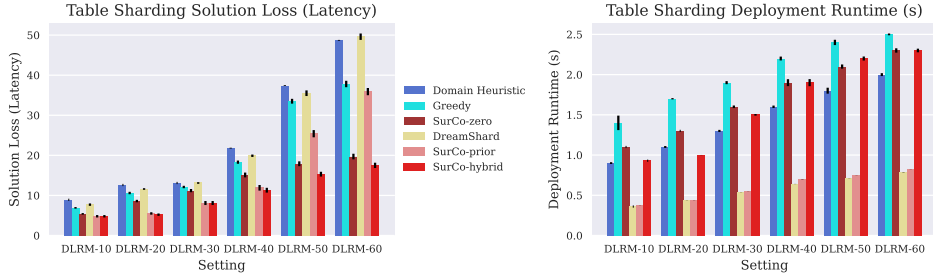


Figure 2: Table placement plan latency (left) and solver runtime (right). We evaluate SurCo against Dreamshard (Zha et al., 2022b), a SoTA offline RL solver, a domain-heuristic of assigning tables based on dimension, and a greedy heuristic based on the runtime increase. Striped approaches require pre-training.

185 **Difference between Cost and Solution Regression.** In the following we will show that in certain
 186 cases, the direct prediction $\mathbf{y} \mapsto \mathbf{x}^*(\mathbf{y})$ could have an infinitely large Lipschitz constant L . To show
 187 this, let us consider a general mapping $\phi : \mathbb{R}^d \supseteq Y \mapsto \mathbb{R}^m$. Let $\phi(Y)$ be the image of Y under
 188 mapping ϕ and $\kappa(Y)$ be the number of connected components for region Y .

189 **Theorem 4.4** (A case of infinite Lipschitz constant). *If the minimal distance d_{\min} for different*
 190 *connected components of $\phi(Y)$ is strictly positive, and $\kappa(\phi(Y)) > \kappa(Y)$, then the Lipschitz constant*
 191 *of the mapping ϕ is infinite.*

192 Note that this theorem applies to a wide variety of combinatorial optimization problems. For
 193 example, when Y is a connected region and the optimization problem can be formulated as an integer
 194 programming, the optimal solution set $\mathbf{x}^*(Y) := \{\mathbf{x}^*(\mathbf{y}) : \mathbf{y} \in Y\}$ is a discrete set of integral
 195 vertices, so the theorem applies. Combined with analysis in Sec. 4, we know the mapping $\mathbf{y} \mapsto \mathbf{x}^*(\mathbf{y})$
 196 is hard to learn even with a lot of samples.

197 We can see this more clearly with a concrete example in 2D space. Let the 1D instance description
 198 $y \in [0, \pi/2]$, and the feasible region is a convex hull of 3 vertices $\{(0, 0), (0, 1), (1, 0)\}$. The
 199 nonlinear objective is simply $f(\mathbf{x}; y) := (x_1 \cos(y) + x_2 \sin(y))^2$, in which $\mathbf{x} = (x_1, x_2)$ is the 2D
 200 solution vector. The direct mapping $y \rightarrow \mathbf{x}^*$ maps a continuous region of instance descriptions (i.e.,
 201 $y \in [0, \pi/2]$) into 2 disjoint regions points ($\mathbf{x}^* = (0, 1)$ and $\mathbf{x}^* = (1, 0)$), and thus according to
 202 Theorem 4.4, its Lipschitz constant must be infinite. In contrast, there exists a surrogate cost mapping
 203 $\mathbf{c}(y) = [\cos(y), \sin(y)]^\top$, and the mapping $y \rightarrow \mathbf{c}$ has finite Lipschitz constant (actually $L \leq 1$) and
 204 can be learned easily.

205 5 Empirical Evaluation

206 We evaluate the variants of SurCo on three settings, embedding table sharding, inverse photonic
 207 design, and nonlinear route planning, with the first two being real-world industrial settings. Each
 208 setting consists of a family of problem instances with varying feasible region and nonlinear objective
 209 function. Additionally, both table sharding and inverse photonic design lack analytical formulations
 210 of the objective function which prevents them from being used by many off-the-shelf nonlinear
 211 solvers like SCIP (Achterberg, 2009).

212 **Embedding Table Sharding.** The task of sharding embedding tables arises in the deployment
 213 of large-scale neural network models which operate over both sparse and dense inputs (e.g., in
 214 recommendation systems (Zha et al., 2022a,b, 2023; Sethi et al., 2022)). Given T embedding tables
 215 and D homogeneous devices, the goal is to distribute the tables among the devices such that no
 216 device’s memory limit is exceeded, while the tables are processed efficiently. Formally, let $x_{t,d}$ be
 217 the binary variable indicating whether table t is assigned to device d , and $\mathbf{x} := \{x_{t,d}\} \in \{0, 1\}^{TD}$
 218 be the collection of the variables. The optimization problem is $\min_{\mathbf{x} \in \Omega} f(\mathbf{x}; \mathbf{y})$ where $\Omega(\mathbf{y}) :=$
 219 $\{\mathbf{x} : \forall t, \sum_d x_{t,d} = 1, \forall d, \sum_t m_t x_{t,d} \leq M\}$.

220 Here the problem description \mathbf{y} includes table memory usage $\{m_t\}$, and capacity M of each device.
 221 $\sum_d x_{t,d} = 1$ means each table t should be assigned to exactly one device, and $\sum_d m_t x_{t,d} \leq M$
 222 means the memory consumption at each device d should not exceed its capacity. The nonlinear
 223 cost function $f(\mathbf{x}; \mathbf{y})$ is the *latency*, i.e., the runtime of the longest-running device. Due to shared
 224 computation (e.g., batching) among the group of assigned tables, and communication costs across
 225 devices, the objective is highly nonlinear. $f(\mathbf{x}; \mathbf{y})$ is well-approximated by a sharding plan runtime
 226 estimator proposed by Dreamshard (Zha et al., 2022b). Note that here, the runtime is approximated
 227 by a differentiable function since the real world deployment runtime isn’t differentiable.

228 SurCo learns to predict $T \times D$ surrogate cost $\hat{c}_{t,d}$, one for each potential table-device assignment.
 229 During training, the gradients through the combinatorial solver $\partial \mathbf{g} / \partial \mathbf{c}$ are computed via CVXPY-
 230 Layers (Agrawal et al., 2019a), and the integrality constraints are relaxed. In practice, we obtained
 231 mostly integral solutions in that only one table on any given device was fractional. At test time, we
 232 solve for the integer solution using SCIP (Achterberg, 2009), a branch and bound MILP solver.

233 **Settings.** We evaluate SurCo on the public Deep Learning Recommendation Model (DLRM)
 234 dataset (Naumov et al., 2019). We consider 6 settings placing 10, 20, 30, 40, 50, and 60 tables on 4
 235 devices, with a 5GB memory limit on GPU devices and 100 instances each (50 train, 50 test).

236 **Baselines.** Greedy allocates tables to devices based on local latency increase f , and the domain-
 237 expert algorithm Domain-Heuristic balances the aggregate dimension (Zha et al., 2022b). For
 238 SurCo-prior, we use Dreamshard, the SoTA embedding table sharding RL algorithm.

239 **Results.** Fig. 2, SurCo-zero finds lower latency sharding plans than the baselines, while it takes
 240 slightly longer than Domain-Heuristic and DreamShard due to taking optimization steps rather
 241 than building a solution with an RL policy. SurCo-prior obtains lower latency solutions in about
 242 the same time as DreamShard with a slight runtime increase from SCIP. Lastly, SurCo-hybrid
 243 obtains the best solutions and has runtime comparable to SurCo-zero. In smaller instances
 244 ($T \leq 40$), SurCo-prior finds better solutions than its impromptu counterpart, SurCo-zero,
 245 likely by escaping local optima by training on a variety of examples. For larger instances with more
 246 tables available for placement, SurCo-zero performs better by optimizing for the test instances as
 247 opposed to SurCo-prior which only uses training data. Using SurCo-hybrid, we obtain the
 248 best solutions but incur the upfront pretraining cost and the deployment-time optimization cost.

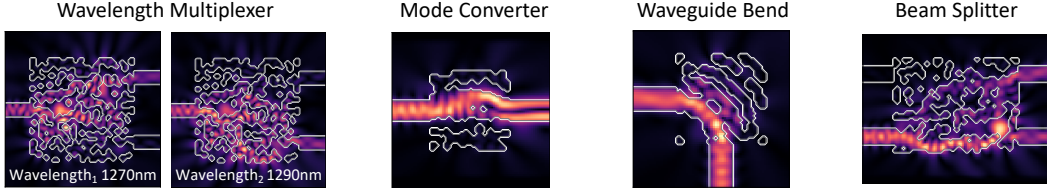


Figure 3: Inverse photonic design settings from the ceviche challenges Schubert et al. (2022) along with SurCo-zero solution designs and wavelength intensities. Light is fed in on the left and is routed at desired intensities to the output by designing the intermediate region. In the Wavelength Multiplexer setting, two wavelengths of interest are visualized as they are routed to different locations.

249 **Inverse Photonic Design.** Photonic devices play an essential role in high-speed communication
 250 (Marpaung et al., 2019), quantum computing (Arazola et al., 2021), and machine learning hardware
 251 acceleration (Wetzstein et al., 2020). The photonic components can be encoded as a binary 2D grid,
 252 with each cell being filled or void. There are constraints on which binary patterns are physically
 253 manufacturable: only those that can be drawn by a physical brush instrument with a specific cross
 254 shape can be manufactured. It remains challenging to find manufacturable designs that satisfy
 255 design specifications like splitting beams of light. An example solution developed by SurCo is
 256 shown in Figure 3: beams are routed from the left to output locations, depending on wavelength.
 257 The solution is also manufacturable: a 3-by-3 cross can fit in all filled and void space. Given the
 258 design, existing work (Hughes et al., 2019) enables differentiation of the design misspecification cost,
 259 evaluated as how far off the transmission intensity of the wavelengths are from the desired output
 260 locations, with zero design loss meaning that the specification is satisfied. Researchers also develop
 261 the Ceviche Challenges (Schubert et al., 2022) a standard benchmark of inverse photonic design
 262 problems. Formally, a feasible design is a rectangle of pixels which are either filled or void where
 263 both the filled and void pixels can be expressed as a unions of the brush shape. Please see (Schubert
 264 et al., 2022) for an in depth description of the nonlinear objective and feasible region.

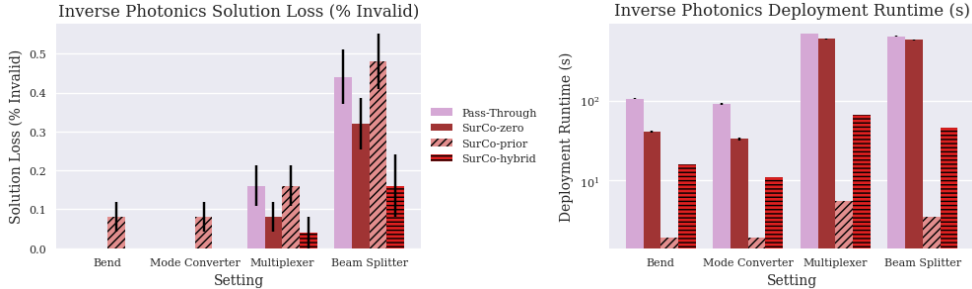


Figure 4: **Left** The solution loss (% of failed instances when the design loss is not 0), and **right** test time solver runtime in log scale. For both, lower is better. We compare against the Pass-Through gradient approach proposed in Schubert et al. (2022). We observe that SurCo-prior achieves similar success rates to the previous approach Pass-Through with a substantially improved runtime. Additionally, SurCo-zero runs comparably or faster, while finding more valid solutions than Pass-Through. SurCo-hybrid obtains valid solutions most often and is faster than SurCo-zero at the expense of pretraining. Striped approaches use pretraining.

265 **Settings.** We compare our approaches against the Pass-Through method (Schubert et al., 2022)
 266 on randomly generated instances of the four types of problems in Schubert et al. (2022): Waveguide
 267 Bend, Mode Converter, Wavelengths Division Multiplexer, and Beam Splitter. We generate 50
 268 instances in each setting (25 training/25 test), randomly sampling the location of input and output
 269 waveguides, or “pipes” where we are taking in light and desire light to output. We fix the wavelengths
 270 themselves and so the problem description y contains an image description of the problem instance,
 271 where each pixel is either “fixed” or “designable”. Further generation details are in the appendix. We
 272 evaluated several algorithms described in the appendix, such as genetic algorithms and derivative-free
 273 optimization, which failed to find feasible solutions. We consider two wavelengths (1270nm/1290nm),
 274 and optimize at a resolution of 40nm, visualizing the test results in Fig. 4.

275 **Results.** Fig. 4, SurCo-zero consistently finds as many or more valid devices compared to the
 276 Pass-Through baseline (Schubert et al., 2022). Additionally, since the on-the-fly solvers stop

277 when they either find a valid solution, or reach a maximum of 200 steps, the runtime of SurCo-zero
 278 is slightly lower than the Pass-Through baseline. SurCo-prior obtains similar success rates as
 279 Pass-Through while taking two orders of magnitude less time as it does not require impromptu
 280 optimization. Lastly, SurCo-hybrid finds valid solutions more often than the other approaches. It
 281 also takes less runtime than the other on-the-fly approaches although it still requires optimization
 282 on-the-fly so it takes longer than SurCo-prior. In Fig. 5, SurCo-zero has smoother and faster
 283 convergence than Pass-Through.

284 **Nonlinear Route Planning.** Nonlinear route
 285 planning can arise where one wants to maxi-
 286 mize the probability of arrival before a set time
 287 in graphs with random edges (Fan et al., 2005;
 288 Nikolova et al., 2006; Lim et al., 2013). These
 289 problems occur in risk-aware settings where oper-
 290 ators need to maximize the probability of ar-
 291 riving before a critical time.

292 Given a graph G with edge lengths coming
 293 from a random distribution, a pair of source
 294 and destination nodes s, t , and a time limit
 295 T that we would like to arrive before, we se-
 296 lect a feasible $s - t$ path $P_{s,t}$ that maximizes
 297 the probability of arriving before the deadline
 298 $P[\text{length}(P_{s,t}) \leq T]$. If we assume that edge
 299 times are distributed according to a random nor-
 300 mal distribution $t_e \sim \mathcal{N}(\mu_e, \sigma_e^2)$, then we could
 301 write the objective as maximizing $f(x; y) =$
 302 $\Phi\left(\frac{(T - \sum_{e \in P_{s,t}} \mu_e) / \sqrt{\sum_{e \in P_{s,t}} \sigma_e^2}}{\sqrt{\sum_{e \in P_{s,t}} \sigma_e^2}}\right)$, with Φ

303 being the cumulative distribution function of a standard Gaussian distribution, with the feasible
 304 region $\Omega(y)$ being the set of $s - t$ paths in the graph. Explicitly, the problem parameters y are the
 305 graph G , source and destination nodes s, t , time limit T , and the edge weight distributions given
 306 by means and variances μ_e, σ_e^2 . We only consider the zero-shot setting since we need to solve the
 307 problem on-the-fly. SurCo trains surrogate edge costs \hat{c}_e , finds the shortest path using Bellman-Ford
 308 (Bellman, 1958), and differentiates using blackbox differentiation (Pogančić et al., 2019).

309 **Settings.** We run on a 5x5 grid graph with 25
 310 draws of edge parameters $\mu_e \sim U(0.1, 1)$ and
 311 $\sigma_e^2 \sim U(0.1, 0.3) * (1 - \mu_e)$, with $U(a, b)$ being
 312 the uniform random distribution between a and
 313 b . We have deadline settings based on the length
 314 of the least expected time path (LET) which is
 315 simply the shortest path using μ_e as weights.
 316 We use loose, normal, and tight deadlines of
 317 1.1 LET, 1 LET, and 0.9 LET respectively. The
 318 source and destination are opposite corners of the
 319 grid graph.

320 **Results.** Fig. 6, we compare SurCo-zero
 321 against a domain-specific approach that mini-
 322 mizes a linear combination of mean and variance
 323 (Nikolova et al., 2006), and SCIP (Achterberg,
 324 2009). In this setting, we focus on the zero-shot
 325 performance of SurCo, comparing it against
 326 two other zero-shot approaches. Furthermore,
 327 here we are able to encode the objective analytically
 328 into SCIP whereas the objectives of the other settings
 329 do not have readily-encodeable formulations, relying
 330 on neural networks or physical simulation. Since SurCo-zero
 331 and the domain approach take much less than 1 second,
 332 we use SCIP-1s and find that SCIP cannot find feasible
 333 solutions at that time scale. SCIP-30min demonstrates
 334 how well a general-purpose method can do given
 335 enough time, with SCIP timing out on all instances.
 336 We also find that SurCo-zero

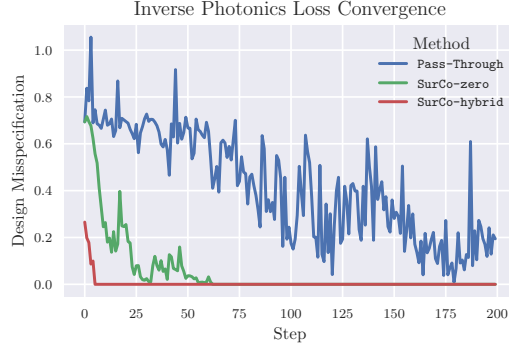


Figure 5: Inverse photonic design convergence. SurCo-zero smoothly lowers the loss while the baseline converges noisily. SurCo-hybrid fine-tunes an already high-quality solution.

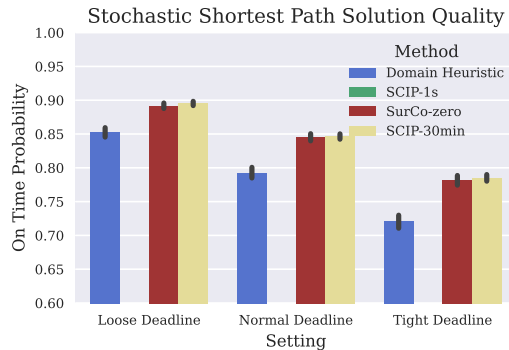


Figure 6: Comparison of nonlinear route planning probability of arriving on time. We compare against a domain heuristic (Nikolova et al., 2006) and SCIP (Achterberg, 2009). SurCo-zero outperforms the domain heuristic, and is similar to SCIP using less time. SCIP-1s fails to find feasible solutions.

333 is able to obtain comparable solutions to SCIP-30min. Furthermore, `SurCo-zero` consistently
334 outperforms the domain heuristic, finding paths that reach the deadline with 4.5%, 6.5%, 8.5% times
335 higher success rates in loose, normal, and tight deadlines. Finally, the domain heuristic only beats
336 `SurCo-zero` in 2 instances.

337 6 Related Work

338 **Differentiable Optimization.** OptNet (Amos & Kolter, 2017) implicitly differentiates through KKT
339 conditions: equations that determine the optimal solution. Followup work differentiated through
340 linear programs (Wilder et al., 2019a), submodular optimization (Djlonga & Krause, 2017; Wilder
341 et al., 2019a; Wang et al., 2020a), cone programs (Agrawal et al., 2019a,b), MaxSAT (Wang et al.,
342 2019), mixed integer linear programs (Ferber et al., 2020; Mandi et al., 2020), integer linear programs
343 (Mandi et al., 2020), dynamic programs Demirovic et al. (2020), blackbox discrete linear optimizers
344 (Pogančić et al., 2019; Rolínek et al., 2020a,b), maximum likelihood estimation (Niepert et al., 2021),
345 kmeans clustering (Wilder et al., 2019b), knapsack (Guler et al., 2022; Demirović et al., 2019), the
346 cross-entropy method (Amos & Yarats, 2020), least squares (Pineda et al., 2022), SVM training (Lee
347 et al., 2019). `SurCo` can use these surrogates as needed.

348 **Task Based Learning.** Task-based learning solves distributions of linear or quadratic optimization
349 problems with the true objective hidden at test time but available for training (Elmachtoub & Grigas,
350 2022b; Donti et al., 2017; El Balghiti et al., 2019; Liu & Grigas, 2021; Hu et al., 2022). (Donti et al.,
351 2021) predicts solutions for continuous nonlinear optimization. Machine learning can also guide
352 combinatorial algorithms. Several approaches produce combinatorial solutions (Zhang & Dieterich,
353 1995; Khalil et al., 2017; Kool et al., 2018; Nazari et al., 2018; Zha et al., 2022a,b), but are limited
354 to constructively building solutions for problems like routing, assignment, or covering. However,
355 these approaches fail to handle more complex constraints. Other approaches set parameters that
356 improve solver runtime (Khalil et al., 2016; Bengio et al., 2021). Similarly, a neural diving approach
357 has been proposed for finding fast MILP solutions Nair et al. (2020), but requires iteratively solving
358 subproblems which are nontrivial for nonlinear objectives.

359 **Learning Latent Space for Optimization.** We learn latent linear objectives to optimize nonlinear
360 functions while other approaches learn latent embeddings for faster solving. FastMap (Faloutsos &
361 Lin, 1995) learns latent embeddings for efficient search, with variants for graph optimization and
362 shortest path (Cohen et al., 2018; Hu et al., 2022; Li et al., 2019). Wang et al. (2020b, 2021a); Yang
363 et al. (2021); Zhao et al. (2022) use Monte Carlo Tree Search to learn to split the search space.

364 **Mixed Integer Nonlinear Programming (MINLP).** `SurCo-zero` solves some MINLP instances,
365 optimizing nonlinear objectives over discrete linear regions, like some general solvers (Burer &
366 Letchford, 2012; Belotti et al., 2013); however, scalability often requires problem-specific techniques.

367 7 Conclusion

368 We introduced `SurCo`, a method for learning linear surrogates for combinatorial nonlinear opti-
369 mization problems. At its core, `SurCo` differentiates through the surrogate solver which maps the
370 predicted coefficients to a combinatorially feasible solution, combining the flexibility of gradient-
371 based optimization with the structure of combinatorial solvers. Our theoretical intuition for `SurCo`
372 poses promising directions for future work in proving convergence guarantees or generalization
373 bounds. We present three variants of `SurCo`, `SurCo-zero` for individual instances, `SurCo-`
374 `prior` which trains a coefficient prediction model offline, and `SurCo-hybrid` which fine-tunes
375 the coefficients predicted by `SurCo-prior` on individual test instances. We evaluated variants of
376 `SurCo` against the state-of-the-art approaches on three domains, with two used in industry, obtaining
377 better solutions faster in the embedding table sharding domain, quickly identifying viable photonic
378 devices, and finding successful routes in stochastic path planning. Overall, `SurCo` trains linear
379 surrogate coefficients to find high-quality solutions to tackle a broad class of combinatorial problems
380 with nonlinear objectives where off-the-shelf solvers fail.

381 **References**

- 382 Achterberg, T. Scip: solving constraint integer programs. *Mathematical Programming Computation*,
383 1(1):1–41, 2009.
- 384 Agrawal, A., Amos, B., Barratt, S., Boyd, S., Diamond, S., and Kolter, J. Z. Differentiable convex
385 optimization layers. *Advances in neural information processing systems*, 32, 2019a.
- 386 Agrawal, A., Barratt, S., Boyd, S., Busseti, E., and Moursi, W. M. Differentiating through a cone
387 program. *J. Appl. Numer. Optim*, 1(2):107–115, 2019b.
- 388 Amos, B. and Kolter, J. Z. Optnet: Differentiable optimization as a layer in neural networks. In
389 *International Conference on Machine Learning*, pp. 136–145. PMLR, 2017.
- 390 Amos, B. and Yarats, D. The differentiable cross-entropy method. In *International Conference on*
391 *Machine Learning*, pp. 291–302. PMLR, 2020.
- 392 Arrazola, J. M., Bergholm, V., Bradler, K., Bromley, T. R., Collins, M. J., Dhand, I., Fumagalli, A.,
393 Gerrits, T., Goussev, A., Helt, L. G., et al. Quantum circuits with many photons on a programmable
394 nanophotonic chip. *Nature*, 591(7848):54–60, 2021.
- 395 Ban, G.-Y. and Rudin, C. The big data newsvendor: Practical insights from machine learning.
396 *Operations Research*, 67(1):90–108, 2019.
- 397 Bellman, R. On a routing problem. *Quarterly of applied mathematics*, 16(1):87–90, 1958.
- 398 Belotti, P., Kirches, C., Leyffer, S., Linderoth, J., Luedtke, J., and Mahajan, A. Mixed-integer
399 nonlinear optimization. *Acta Numerica*, 22:1–131, 2013.
- 400 Bengio, Y., Lodi, A., and Prouvost, A. Machine learning for combinatorial optimization: a method-
401 ological tour d’horizon. *European Journal of Operational Research*, 290(2):405–421, 2021.
- 402 Berthet, Q., Blondel, M., Teboul, O., Cuturi, M., Vert, J.-P., and Bach, F. Learning with differentiable
403 perturbed optimizers. *Advances in neural information processing systems*, 33:9508–9519, 2020.
- 404 Bradbury, J., Frostig, R., Hawkins, P., Johnson, M. J., Leary, C., Maclaurin, D., Necula, G., Paszke,
405 A., VanderPlas, J., Wanderman-Milne, S., and Zhang, Q. JAX: composable transformations of
406 Python+NumPy programs, 2018. URL <http://github.com/google/jax>.
- 407 Burer, S. and Letchford, A. N. Non-convex mixed-integer nonlinear programming: A survey. *Surveys*
408 *in Operations Research and Management Science*, 17(2):97–106, 2012.
- 409 Chvatal, V., Chvatal, V., et al. *Linear programming*. Macmillan, 1983.
- 410 Cohen, L., Uras, T., Jahangiri, S., Arunasalam, A., Koenig, S., and Kumar, T. S. The fastmap
411 algorithm for shortest path computations. In *IJCAI*, 2018.
- 412 Cozad, A., Sahinidis, N. V., and Miller, D. C. Learning surrogate models for simulation-based
413 optimization. *AIChE Journal*, 60(6):2211–2227, 2014.
- 414 Demirović, E., J Stuckey, P., Bailey, J., Chan, J., Leckie, C., Ramamohanarao, K., and Guns, T.
415 Predict+ optimise with ranking objectives: Exhaustively learning linear functions. In *Proceed-*
416 *ings of the Twenty-Eighth International Joint Conference on Artificial Intelligence, IJCAI 2019,*
417 *Macao, China, August 10-16, 2019*, pp. 1078–1085. International Joint Conferences on Artificial
418 Intelligence, 2019.
- 419 Demirovic, E., J Stuckey, P., Guns, T., Bailey, J., Leckie, C., Ramamohanarao, K., and Chan, J.
420 Dynamic programming for predict+ optimise. In *The Thirty-Fourth AAAI Conference on Artificial*
421 *Intelligence, AAAI 2020, The Thirty-Second Innovative Applications of Artificial Intelligence Con-*
422 *ference, IAAI 2020, The Tenth AAAI Symposium on Educational Advances in Artificial Intelligence,*
423 *EAAI 2020, New York, NY, USA, February 7-12, 2020*, pp. 1444–1451. AAAI Press, 2020.
- 424 Djolonga, J. and Krause, A. Differentiable learning of submodular models. *Advances in Neural*
425 *Information Processing Systems*, 30, 2017.

- 426 Donti, P., Amos, B., and Kolter, J. Z. Task-based end-to-end model learning in stochastic optimization.
427 *Advances in neural information processing systems*, 30, 2017.
- 428 Donti, P. L., Rolnick, D., and Kolter, J. Z. DC3: A learning method for optimization with hard
429 constraints. In *International Conference on Learning Representations*, 2021. URL <https://openreview.net/forum?id=V1ZHVxJ6dSS>.
430
- 431 El Balghiti, O., Elmachtoub, A. N., Grigas, P., and Tewari, A. Generalization bounds in the predict-
432 then-optimize framework. *Advances in neural information processing systems*, 32, 2019.
- 433 Elmachtoub, A. N. and Grigas, P. Smart “predict, then optimize”. *Management Science*, 68(1):9–26,
434 2022a.
- 435 Elmachtoub, A. N. and Grigas, P. Smart “predict, then optimize”. *Management Science*, 68(1):9–26,
436 2022b.
- 437 Faloutsos, C. and Lin, K.-I. Fastmap: A fast algorithm for indexing, data-mining and visualization
438 of traditional and multimedia datasets. In *Proceedings of the 1995 ACM SIGMOD International
439 Conference on Management of Data*, SIGMOD ’95, pp. 163–174, New York, NY, USA, 1995.
440 Association for Computing Machinery. ISBN 0897917316. doi: 10.1145/223784.223812. URL
441 <https://doi.org/10.1145/223784.223812>.
- 442 Fan, Y., Kalaba, R. E., and Moore, J. E. Arriving on time. *Journal of Optimization Theory and
443 Applications*, 127:497–513, 2005.
- 444 Ferber, A., Wilder, B., Dilkina, B., and Tambe, M. Mipaal: Mixed integer program as a layer. In
445 *Proceedings of the AAAI Conference on Artificial Intelligence*, volume 34, pp. 1504–1511, 2020.
- 446 Fix, E. *Discriminatory analysis: nonparametric discrimination, consistency properties*, volume 1.
447 USAF school of Aviation Medicine, 1985.
- 448 Gad, A. F. Pygad: An intuitive genetic algorithm python library, 2021.
- 449 Gosavi, A. et al. *Simulation-based optimization*. Springer, 2015.
- 450 Guler, A. U., Demirović, E., Chan, J., Bailey, J., Leckie, C., and Stuckey, P. J. A divide and conquer
451 algorithm for predict+ optimize with non-convex problems. In *Proceedings of the AAAI Conference
452 on Artificial Intelligence*, volume 36, pp. 3749–3757, 2022.
- 453 Gurobi Optimization, LLC. Gurobi Optimizer Reference Manual, 2022. URL <https://www.gurobi.com>.
454
- 455 Hu, Y., Kallus, N., and Mao, X. Fast rates for contextual linear optimization. *Management Science*,
456 2022.
- 457 Hughes, T. W., Williamson, I. A., Minkov, M., and Fan, S. Forward-mode differentiation of maxwell’s
458 equations. *ACS Photonics*, 6(11):3010–3016, 2019.
- 459 Jumper, J., Evans, R., Pritzel, A., Green, T., Figurnov, M., Ronneberger, O., Tunyasuvunakool,
460 K., Bates, R., Žídek, A., Potapenko, A., et al. Highly accurate protein structure prediction with
461 alphafold. *Nature*, 596(7873):583–589, 2021.
- 462 Khalil, E., Le Bodic, P., Song, L., Nemhauser, G., and Dilkina, B. Learning to branch in mixed
463 integer programming. In *Proceedings of the AAAI Conference on Artificial Intelligence*, volume 30,
464 2016.
- 465 Khalil, E., Dai, H., Zhang, Y., Dilkina, B., and Song, L. Learning combinatorial optimization
466 algorithms over graphs. *Advances in neural information processing systems*, 30, 2017.
- 467 Kool, W., van Hoof, H., and Welling, M. Attention, learn to solve routing problems! In *International
468 Conference on Learning Representations*, 2018.
- 469 Korte, B. and Hausmann, D. An analysis of the greedy heuristic for independence systems. In *Annals
470 of Discrete Mathematics*, volume 2, pp. 65–74. Elsevier, 1978.

- 471 Koziel, S., Çalık, N., Mahouti, P., and Belen, M. A. Accurate modeling of antenna structures
472 by means of domain confinement and pyramidal deep neural networks. *IEEE Transactions on*
473 *Antennas and Propagation*, 70(3):2174–2188, 2021.
- 474 Land, A. H. and Doig, A. G. An automatic method for solving discrete programming problems. In
475 *50 Years of Integer Programming 1958-2008*, pp. 105–132. Springer, 2010.
- 476 Lee, K., Maji, S., Ravichandran, A., and Soatto, S. Meta-learning with differentiable convex
477 optimization. In *Proceedings of the IEEE/CVF conference on computer vision and pattern*
478 *recognition*, pp. 10657–10665, 2019.
- 479 Li, J., Felner, A., Koenig, S., and Kumar, T. S. Using fastmap to solve graph problems in a euclidean
480 space. In *Proceedings of the international conference on automated planning and scheduling*,
481 volume 29, pp. 273–278, 2019.
- 482 Li, S., Yan, Z., and Wu, C. Learning to delegate for large-scale vehicle routing. *Advances in Neural*
483 *Information Processing Systems*, 34:26198–26211, 2021.
- 484 Li, Z., Chen, Q., and Koltun, V. Combinatorial optimization with graph convolutional networks and
485 guided tree search. *Advances in neural information processing systems*, 31, 2018.
- 486 Lim, S., Sommer, C., Nikolova, E., and Rus, D. Practical route planning under delay uncertainty:
487 Stochastic shortest path queries. In *Robotics: Science and Systems*, volume 8, pp. 249–256. United
488 States, 2013.
- 489 Liu, H. and Grigas, P. Risk bounds and calibration for a smart predict-then-optimize method.
490 *Advances in Neural Information Processing Systems*, 34:22083–22094, 2021.
- 491 Liuzzi, G., Lucidi, S., and Rinaldi, F. Derivative-free methods for mixed-integer constrained
492 optimization problems. *Journal of Optimization Theory and Applications*, 164(3):933–965, 2015.
- 493 Mandi, J., Stuckey, P. J., Guns, T., et al. Smart predict-and-optimize for hard combinatorial optimiza-
494 tion problems. In *Proceedings of the AAAI Conference on Artificial Intelligence*, volume 34, pp.
495 1603–1610, 2020.
- 496 Marpaung, D., Yao, J., and Capmany, J. Integrated microwave photonics. *Nature photonics*, 13(2):
497 80–90, 2019.
- 498 Mazyavkina, N., Sviridov, S., Ivanov, S., and Burnaev, E. Reinforcement learning for combinatorial
499 optimization: A survey. *Computers & Operations Research*, 134:105400, 2021.
- 500 Mirhoseini, A., Goldie, A., Yazgan, M., Jiang, J. W., Songhori, E., Wang, S., Lee, Y.-J., Johnson,
501 E., Pathak, O., Nazi, A., et al. A graph placement methodology for fast chip design. *Nature*, 594
502 (7862):207–212, 2021.
- 503 Nagai, R., Akashi, R., and Sugino, O. Completing density functional theory by machine learning
504 hidden messages from molecules. *npj Computational Materials*, 6(1):1–8, 2020.
- 505 Nair, V., Bartunov, S., Gimeno, F., Von Glehn, I., Lichocki, P., Lobov, I., O’Donoghue, B., Sonnerat,
506 N., Tjandraatmadja, C., Wang, P., et al. Solving mixed integer programs using neural networks.
507 *arXiv preprint arXiv:2012.13349*, 2020.
- 508 Naumov, M., Mudigere, D., Shi, H. M., Huang, J., Sundaraman, N., Park, J., Wang, X., Gupta, U.,
509 Wu, C., Azzolini, A. G., Dzhuulgakov, D., Mallevich, A., Cherniavskii, I., Lu, Y., Krishnamoorthi,
510 R., Yu, A., Kondratenko, V., Pereira, S., Chen, X., Chen, W., Rao, V., Jia, B., Xiong, L., and
511 Smelyanskiy, M. Deep learning recommendation model for personalization and recommendation
512 systems. *CoRR*, abs/1906.00091, 2019. URL <https://arxiv.org/abs/1906.00091>.
- 513 Nazari, M., Oroojlooy, A., Snyder, L., and Takác, M. Reinforcement learning for solving the vehicle
514 routing problem. *Advances in neural information processing systems*, 31, 2018.
- 515 Niepert, M., Minervini, P., and Franceschi, L. Implicit mle: backpropagating through discrete
516 exponential family distributions. *Advances in Neural Information Processing Systems*, 34:14567–
517 14579, 2021.

- 518 Nikolova, E., Kelner, J. A., Brand, M., and Mitzenmacher, M. Stochastic shortest paths via quasi-
519 convex maximization. In *European Symposium on Algorithms*, pp. 552–563. Springer, 2006.
- 520 Paszke, A., Gross, S., Massa, F., Lerer, A., Bradbury, J., Chanan, G., Killeen, T., Lin, Z., Gimelshein,
521 N., Antiga, L., Desmaison, A., Kopf, A., Yang, E., DeVito, Z., Raison, M., Tejani, A., Chilamkurthy,
522 S., Steiner, B., Fang, L., Bai, J., and Chintala, S. Pytorch: An imperative style, high-performance
523 deep learning library. In Wallach, H., Larochelle, H., Beygelzimer, A., d'Alché-Buc, F., Fox, E.,
524 and Garnett, R. (eds.), *Advances in Neural Information Processing Systems 32*, pp. 8024–8035.
525 Curran Associates, Inc., 2019.
- 526 Pineda, L., Fan, T., Monge, M., Venkataraman, S., Sodhi, P., Chen, R. T., Ortiz, J., DeTone, D., Wang,
527 A., Anderson, S., et al. Theseus: A library for differentiable nonlinear optimization. *Advances in
528 Neural Information Processing Systems*, 35:3801–3818, 2022.
- 529 Pogančić, M. V., Paulus, A., Musil, V., Martius, G., and Rolinek, M. Differentiation of blackbox
530 combinatorial solvers. In *International Conference on Learning Representations*, 2019.
- 531 Rapin, J. and Teytaud, O. Nevergrad - A gradient-free optimization platform. <https://GitHub.com/FacebookResearch/Nevergrad>, 2018.
532
- 533 Reingold, E. M. and Tarjan, R. E. On a greedy heuristic for complete matching. *SIAM Journal on
534 Computing*, 10(4):676–681, 1981.
- 535 Rolínek, M., Musil, V., Paulus, A., Vlastelica, M., Michaelis, C., and Martius, G. Optimizing
536 rank-based metrics with blackbox differentiation. In *Proceedings of the IEEE/CVF Conference on
537 Computer Vision and Pattern Recognition*, pp. 7620–7630, 2020a.
- 538 Rolínek, M., Swoboda, P., Zietlow, D., Paulus, A., Musil, V., and Martius, G. Deep graph matching
539 via blackbox differentiation of combinatorial solvers. In *European Conference on Computer Vision*,
540 pp. 407–424. Springer, 2020b.
- 541 Ruder, S. An overview of gradient descent optimization algorithms. *arXiv preprint arXiv:1609.04747*,
542 2016.
- 543 Schubert, M. F., Cheung, A. K. C., Williamson, I. A. D., Spyra, A., and Alexander, D. H. Inverse
544 design of photonic devices with strict foundry fabrication constraints. *ACS Photonics*, 9(7):
545 2327–2336, 2022. doi: 10.1021/acsp Photonics.2c00313.
- 546 Sethi, G., Acun, B., Agarwal, N., Kozyrakis, C., Trippel, C., and Wu, C.-J. Recshard: statistical
547 feature-based memory optimization for industry-scale neural recommendation. In *Proceedings of
548 the 27th ACM International Conference on Architectural Support for Programming Languages
549 and Operating Systems*, pp. 344–358, 2022.
- 550 Simon, D. *Evolutionary optimization algorithms*. John Wiley & Sons, 2013.
- 551 Steiner, B., Cummins, C., He, H., and Leather, H. Value learning for throughput optimization of
552 deep learning workloads. In Smola, A., Dimakis, A., and Stoica, I. (eds.), *Proceedings of Machine
553 Learning and Systems*, volume 3, pp. 323–334, 2021. URL <https://proceedings.mlsys.org/paper/2021/file/73278a4a86960eeb576a8fd4c9ec6997-Paper.pdf>.
554
- 555 Van Rossum, G. and Drake, F. L. *Python 3 Reference Manual*. CreateSpace, Scotts Valley, CA, 2009.
556 ISBN 1441412697.
- 557 Vaswani, A., Shazeer, N., Parmar, N., Uszkoreit, J., Jones, L., Gomez, A. N., Kaiser, Ł., and
558 Polosukhin, I. Attention is all you need. *Advances in neural information processing systems*, 30,
559 2017.
- 560 Voß, S., Martello, S., Osman, I. H., and Roucairol, C. *Meta-heuristics: Advances and trends in local
561 search paradigms for optimization*. Springer Science & Business Media, 2012.
- 562 Wang, K., Wilder, B., Perrault, A., and Tambe, M. Automatically learning compact quality-aware
563 surrogates for optimization problems. *Advances in Neural Information Processing Systems*, 33:
564 9586–9596, 2020a.

- 565 Wang, L., Fonseca, R., and Tian, Y. Learning search space partition for black-box optimization using
566 monte carlo tree search. *Advances in Neural Information Processing Systems*, 33:19511–19522,
567 2020b.
- 568 Wang, L., Xie, S., Li, T., Fonseca, R., and Tian, Y. Sample-efficient neural architecture search by
569 learning actions for monte carlo tree search. *IEEE Transactions on Pattern Analysis and Machine
570 Intelligence*, 2021a.
- 571 Wang, P.-W., Donti, P., Wilder, B., and Kolter, Z. Satnet: Bridging deep learning and logical reasoning
572 using a differentiable satisfiability solver. In *International Conference on Machine Learning*, pp.
573 6545–6554. PMLR, 2019.
- 574 Wang, X., Liu, Y., Zhao, J., Liu, C., Liu, J., and Yan, J. Surrogate model enabled deep reinforcement
575 learning for hybrid energy community operation. *Applied Energy*, 289:116722, 2021b.
- 576 Wetzstein, G., Ozcan, A., Gigan, S., Fan, S., Englund, D., Soljačić, M., Denz, C., Miller, D. A., and
577 Psaltis, D. Inference in artificial intelligence with deep optics and photonics. *Nature*, 588(7836):
578 39–47, 2020.
- 579 Wilder, B., Dilkina, B., and Tambe, M. Melding the data-decisions pipeline: Decision-focused
580 learning for combinatorial optimization. In *Proceedings of the AAAI Conference on Artificial
581 Intelligence*, volume 33, pp. 1658–1665, 2019a.
- 582 Wilder, B., Ewing, E., Dilkina, B., and Tambe, M. End to end learning and optimization on graphs.
583 *Advances in Neural Information Processing Systems*, 32, 2019b.
- 584 Wolsey, L. A. An analysis of the greedy algorithm for the submodular set covering problem.
585 *Combinatorica*, 2(4):385–393, 1982.
- 586 Wolsey, L. A. Mixed integer programming. *Wiley Encyclopedia of Computer Science and Engineering*,
587 pp. 1–10, 2007.
- 588 Yang, K., Zhang, T., Cummins, C., Cui, B., Steiner, B., Wang, L., Gonzalez, J. E., Klein, D., and
589 Tian, Y. Learning space partitions for path planning. *Advances in Neural Information Processing
590 Systems*, 34:378–391, 2021.
- 591 Ye, Y., Zhang, X., and Sun, J. Automated vehicle’s behavior decision making using deep rein-
592 forcement learning and high-fidelity simulation environment. *Transportation Research Part C:
593 Emerging Technologies*, 107:155–170, 2019.
- 594 Zha, D., Feng, L., Bhushanam, B., Choudhary, D., Nie, J., Tian, Y., Chae, J., Ma, Y., Kejariwal,
595 A., and Hu, X. Autoshard: Automated embedding table sharding for recommender systems. In
596 *Proceedings of the 28th ACM SIGKDD Conference on Knowledge Discovery and Data Mining*, pp.
597 4461–4471, 2022a.
- 598 Zha, D., Feng, L., Tan, Q., Liu, Z., Lai, K.-H., Bhargav, B., Tian, Y., Kejariwal, A., and Hu, X.
599 Dreamshard: Generalizable embedding table placement for recommender systems. In *Advances in
600 Neural Information Processing Systems*, 2022b.
- 601 Zha, D., Feng, L., Luo, L., Bhushanam, B., Liu, Z., Hu, Y., Nie, J., Huang, Y., Tian, Y., Kejariwal, A.,
602 et al. Pre-train and search: Efficient embedding table sharding with pre-trained neural cost models.
603 In *Sixth Conference on Machine Learning and Systems*, 2023.
- 604 Zhang, W. and Dietterich, T. G. A reinforcement learning approach to job-shop scheduling. In *IJCAI*,
605 volume 95, pp. 1114–1120. Citeseer, 1995.
- 606 Zhao, Y., Wang, L., Yang, K., Zhang, T., Guo, T., and Tian, Y. Multi-objective optimization by
607 learning space partition. In *International Conference on Learning Representations*, 2022. URL
608 <https://openreview.net/forum?id=FlwzVjfMryn>.
- 609 Zhou, Y., Roy, S., Abdolrashidi, A., Wong, D., Ma, P., Xu, Q., Liu, H., Phothilimtha, P., Wang, S.,
610 Goldie, A., et al. Transferable graph optimizers for ml compilers. *Advances in Neural Information
611 Processing Systems*, 33:13844–13855, 2020.

612 **A Proofs**

613 **Lemma A.1** (Sufficient condition of prediction with ϵ -accuracy). *If the dataset \mathcal{C} can (ϵ/L) -cover Y ,*
 614 *then for any $\mathbf{y} \in Y$, a 1-nearest-neighbor regressor $\hat{\phi}$ leads to $\|\hat{\phi}(\mathbf{y}) - \phi(\mathbf{y})\|_2 \leq \epsilon$.*

615 *Proof.* Since the dataset is a ϵ/L -cover, for any $\mathbf{y} \in Y$, there exists at least one \mathbf{y}_i so that $\|\mathbf{y} - \mathbf{y}_i\|_2 \leq$
 616 ϵ/L . Let \mathbf{y}_{nn} be the nearest neighbor of \mathbf{y} , and we have:

$$\|\mathbf{y} - \mathbf{y}_{\text{nn}}\|_2 \leq \|\mathbf{y} - \mathbf{y}_i\|_2 \leq \epsilon/L \quad (6)$$

617 From the Lipschitz condition and the definition of 1-nearest-neighbor classifier ($\hat{\phi}(\mathbf{y}) = \phi(\mathbf{y}_{\text{nn}})$),
 618 we know that

$$\|\phi(\mathbf{y}) - \hat{\phi}(\mathbf{y})\|_2 = \|\phi(\mathbf{y}) - \phi(\mathbf{y}_{\text{nn}})\|_2 \leq L\|\mathbf{y} - \mathbf{y}_{\text{nn}}\|_2 \leq \epsilon \quad (7)$$

619 \square

620 **Lemma A.2** (Lower bound of sample complexity for ϵ/L -cover). *To achieve ϵ/L -cover of Y , the size*
 621 *of the dataset set $N \geq N_0(\epsilon) := \frac{\text{vol}(Y)}{\text{vol}_0} \left(\frac{L}{\epsilon}\right)^d$, where vol_0 is the volume of unit ball in d -dimension.*

622 *Proof.* We prove by contradiction. If $N < N_0(\epsilon)$, then for each training sample (\mathbf{y}_i, ϕ_i) , we create a
 623 ball $B_i := B(\mathbf{y}_i, \epsilon/L)$. Since

$$\text{vol}\left(\bigcup_{i=1}^N B_i \cap Y\right) \leq \text{vol}\left(\bigcup_{i=1}^N B_i\right) \leq \sum_{i=1}^N \text{vol}(B_i) = N \text{vol}_0 \left(\frac{\epsilon}{L}\right)^d < \text{vol}(Y) \quad (8)$$

624 Therefore, there exists at least one $\mathbf{y} \in Y$ so that $\mathbf{y} \notin B_i$ for any $1 \leq i \leq N$. This means that \mathbf{y} is
 625 not ϵ/L -covered. \square

626 **Theorem 4.4** (A case of infinite Lipschitz constant). *If the minimal distance d_{\min} for different*
 627 *connected components of $\phi(Y)$ is strictly positive, and $\kappa(\phi(Y)) > \kappa(Y)$, then the Lipschitz constant*
 628 *of the mapping ϕ is infinite.*

629 *Proof.* Let R_1, R_2, \dots, R_K be the $K = \kappa(\phi(Y))$ connected components of $\phi(Y)$, and
 630 Y_1, Y_2, \dots, Y_J be the $J = \kappa(Y)$ connected components of Y . From the condition, we know
 631 that $\min_{k \neq k'} \text{dist}(R_k, R_{k'}) = d_{\min} > 0$.

632 We have $R_k \cap R_{k'} = \emptyset$ for $k \neq k'$. Each R_k has a pre-image $S_k := \phi^{-1}(R_k) \subseteq Y$. These
 633 pre-images $\{S_k\}_{k=1}^K$ form a partition of Y since

- 634 • $S_k \cap S_{k'} = \emptyset$ for $k \neq k'$ since any $\mathbf{y} \in Y$ cannot be mapped to more than one connected
 635 components;
- 636 • $\bigcup_{k=1}^K S_k = \bigcup_{k=1}^K \phi^{-1}(R_k) = \phi^{-1}\left(\bigcup_{k=1}^K R_k\right) = \phi^{-1}(\phi(S)) = S$.

637 Since $K = \kappa(\phi(Y)) > \kappa(Y)$, by pigeonhole principle, there exists one Y_j that contains at least part
 638 of the two pre-images S_k and $S_{k'}$ with $k \neq k'$. This means that

$$S_k \cap Y_j \neq \emptyset, \quad S_{k'} \cap Y_j \neq \emptyset \quad (9)$$

639 Then we pick $\mathbf{y} \in S_k \cap Y_j$ and $\mathbf{y}' \in S_{k'} \cap Y_j$. Since $\mathbf{y}, \mathbf{y}' \in Y_j$ and Y_j is a connected component,
 640 there exists a continuous path $\gamma : [0, 1] \mapsto Y_j$ so that $\gamma(0) = \mathbf{y}$ and $\gamma(1) = \mathbf{y}'$. Therefore, we have
 641 $\phi(\gamma(0)) \in R_k$ and $\phi(\gamma(1)) \in R_{k'}$. Let $t_0 := \sup\{t : t \in [0, 1], \phi(\gamma(t)) \in R_k\}$, then $0 \leq t_0 < 1$.
 642 For any sufficiently small $\epsilon > 0$, we have:

- 643 • By the definition of sup, we know there exists $t_0 - \epsilon \leq t' \leq t_0$ so that $\phi(\gamma(t')) \in R_k$.
- 644 • Picking $t'' = t_0 + \epsilon < 1$, then $\phi(\gamma(t'')) \in R_{k'}$ with some $k'' \neq k$.

645 On the other hand, by continuity of the curve γ , there exists a constant $C(t_0)$ so that $\|\gamma(t') -$
 646 $\gamma(t'')\|_2 \leq C(t_0)\|t' - t''\|_2 \leq 2C(t_0)\epsilon$. Then we have

$$L = \max_{\mathbf{y}, \mathbf{y}' \in Y} \frac{\|\phi(\mathbf{y}) - \phi(\mathbf{y}')\|_2}{\|\mathbf{y} - \mathbf{y}'\|_2} \geq \frac{\|\phi(\gamma(t')) - \phi(\gamma(t''))\|_2}{\|\gamma(t') - \gamma(t'')\|_2} \geq \frac{d_{\min}}{2C(t_0)\epsilon} \rightarrow +\infty \quad (10)$$

647 \square

Task	Randomization
mode converter	randomize the right and left waveguide width
bend setting	randomize the waveguide width and length
beam splitter	randomize the waveguide separation, width and length
wavelength division multiplexer	randomize the input and output waveguide locations

Table 2: Task randomization of 4 different tasks in inverse photonic design.

648 B Experiment Details

649 B.1 Setups

650 Experiments are performed on a cluster of identical machines, each with 4 Nvidia A100 GPUs and
651 32 CPU cores, with 1T of RAM and 40GB of GPU memory. Additionally, we perform all operations
652 in Python (Van Rossum & Drake, 2009) using Pytorch (Paszke et al., 2019). For embedding
653 table placement, the nonlinear cost estimator is trained for 200 iterations and the offline-trained
654 models of Dreamshard and SurCo-prior are trained against the pretrained cost estimator for
655 200 iterations. The DLRM Dataset Naumov et al. (2019) is available at https://github.com/facebookresearch/dlrm_datasets, and the dreamshard (Zha et al., 2022b) code
656 is available at <https://github.com/daochenzha/dreamshard>. Additional details on
657 dreamshard’s model architecture and features can be obtained in the paper and codebase. Training
658 time for the networks used in SurCo-prior and SurCo-hybrid are on average 8 hours for the
659 inverse photonic design settings and 6, 21, 39, 44, 50, 63 minutes for DLRM 10, 20, 30, 40, 50, 60
660 settings respectively.
661

662 B.2 Network Architectures

663 B.2.1 Embedding Table Sharding

664 The table features are the same used in Zha et al. (2022b), and sinusoidal positional encoding Vaswani
665 et al. (2017) is used as device features so that the learning model is able to break symmetries between
666 the different tables and effectively group them onto homogeneous devices. The table and device
667 features are concatenated and then fed into Dreamshard’s initial fully-connected table encoding
668 module to obtain scalar predictions $\hat{c}_{t,d}$ for each desired objective coefficient. The architecture is
669 trained with the Adam optimizer with learning rate 0.0005. Here, we use the dreamshard backbone to
670 predict coefficients for each table-device pair. We add more output dimensions to the dreamshard
671 backbone, ensuring that we output the desired number of coefficients.

672 B.2.2 Inverse Photonic Design

673 **Network architectures.** The input design specification (a 2D image) is passed through a 3 layer
674 convolutional neural network with ReLU activations and a final layer composed of filtering with the
675 known brush shape. Then a tanh activation is used to obtain surrogate coefficients \hat{c} , one component
676 for each binary input variable. The architecture is trained with the Adam optimizer with learning rate
677 0.001.

678 This is motivated by previous work (Schubert et al., 2022) that also uses the fixed brush shape filter
679 and tanh operation to transform the latent parameters into a continuous solution that is projected onto
680 the space of physically feasible solutions.

681 In each setting, optimization is done on a binary grid of different sizes to meet fabrication constraints,
682 namely that a 3 by 3 cross must fit inside each fixed and void location. In the beam splitter the design
683 is an 80×60 grid, in mode converter it is a 40×40 grid, in waveguide bend it is a 40×40 grid, in
684 wavelength division multiplexer it is an 80×80 grid.

685 Previous work formulated the projection as finding a discrete solution that minimized the dot product
686 of the input continuous solution and proposed discrete solution. The authors then updated the
687 continuous solution by computing gradients of the loss with respect to the discrete solution and using
688 pass-through gradients to update the continuous solution. By comparison, our approach treats the

689 projection as an optimization problem and updates the objective coefficients so that the resulting
 690 projected solution moves in the direction of the desired gradient.

691 To compute the gradient of this blackbox projection solver, we leverage the approach suggested by
 692 Pogančić et al. (2019) which calls the solver twice, once with the original coefficients, and again with
 693 coefficients that are perturbed in the direction of the incoming solution gradient as being an “improved
 694 solution”. The gradient with respect to the input coefficients are then the difference between the
 695 “improved solution” and the solution for the current objective coefficients.

696 C Pseudocode

697 Here is the pseudocode for the different variants of our algorithm. Each of these leverage a differen-
 698 tiable optimization solver to differentiate through the surrogate optimization problem.

Algorithm 1 SurCo-zero

Input: feasible region Ω , data \mathbf{y} , objective f
 $\mathbf{c} \leftarrow \text{init_surrogate_coefs}(\mathbf{y})$
while not converged **do**
 $\mathbf{x} \leftarrow \arg \min_{\mathbf{x} \in \Omega(\mathbf{y})} \mathbf{c}^\top \mathbf{x}$
 $\text{loss} \leftarrow f(\mathbf{x}; \mathbf{y})$
 $\mathbf{c} \leftarrow \text{grad_update}(\mathbf{c}, \nabla_{\mathbf{c}} \text{loss})$
end while
 Return \mathbf{x}

Algorithm 2 SurCo-prior Training

Input: feasible region Ω , data $\mathcal{D}_{\text{train}} = \{\mathbf{y}_i\}_{i=1}^N$, objective f
 $\theta \leftarrow \text{init_surrogate_model}()$
while not converged **do**
 Sample batch $B = \{\mathbf{y}_i\}_i^k \sim \mathcal{D}_{\text{train}}$
for $\mathbf{y} \in B$ **do**
 $\hat{\mathbf{c}} \leftarrow \hat{\mathbf{c}}(\mathbf{y}; \theta)$
 $\mathbf{x} \leftarrow \arg \min_{\mathbf{x} \in \Omega(\mathbf{y})} \mathbf{c}^\top \mathbf{x}$
 $\text{loss} += f(\mathbf{x}; \mathbf{y})$
end for
 $\theta \leftarrow \text{grad_update}(\theta, \nabla_{\theta} \text{loss})$
end while
 Return θ

Algorithm 3 SurCo-prior Deployment

- 1: **Input:** feasible region Ω , data $\mathcal{D}_{\text{train}} = \{\mathbf{y}_i\}_{i=1}^N$, objective f , test instance \mathbf{y}_{test}
- 2: $\theta \leftarrow \text{train_SurCo-prior}(\Omega, \mathcal{D}_{\text{train}}, f)$
- 3: $\mathbf{c} \leftarrow \hat{\mathbf{c}}(\mathbf{y}; \theta)$
- 4: $\mathbf{x} \leftarrow \arg \min_{\mathbf{x} \in \Omega(\mathbf{y})} \mathbf{c}^\top \mathbf{x}$
- 5: Return \mathbf{x}

Algorithm 4 SurCo-hybrid

```
1: Input: feasible region  $\Omega$ , data  $\mathcal{D}_{\text{train}} = \{\mathbf{y}_i\}_{i=1}^N$ , objective  $f$ , test instance  $\mathbf{y}_{\text{test}}$ 
2:  $\theta \leftarrow \text{train\_SurCo\_prior}(\Omega, \mathcal{D}_{\text{train}}, f)$ 
3:  $\mathbf{c} \leftarrow \hat{\mathbf{c}}(\mathbf{y}; \theta)$ 
4: while not converged do
5:    $\mathbf{x} \leftarrow \arg \min_{\mathbf{x} \in \Omega(\mathbf{y})} \mathbf{c}^\top \mathbf{x}$ 
6:   loss  $\leftarrow f(\mathbf{x}; \mathbf{y})$ 
7:    $\mathbf{c} \leftarrow \text{grad\_update}(\mathbf{c}, \nabla_{\mathbf{c}} \text{loss})$ 
8: end while
9: Return  $\mathbf{x}$ 
```

D Additional Failed Baselines

699 **SOGA - Single Objective Genetic Algorithm** Using PyGAD (Gad, 2021), we attempted several
700 approaches for both table sharding and inverse photonics settings. While we were able to obtain
701 feasible table sharding solutions, they underperformed the greedy baseline by 20%. Additionally,
702 they were unable to find physically feasible inverse photonics solutions. We varied between random,
703 swap, inversion, and scramble mutations and used all parent selection methods but were unable to
704 find viable solutions.
705

706 **DFL - A Derivative-Free Library** We could not easily integrate DFLGEN (Liuzzi et al., 2015)
707 into our pipelines since it operates in fortran and we needed to specify the feasible region with
708 python in the ceviche challenges. DFLINT works in python but took more than 24 hours to run on
709 individual instances which reached a timeout limit. We found that the much longer runtime made this
710 inapplicable for the domains of interest.

711 **Nevergrad** We enforced integrality in Nevergrad (Rapin & Teytaud, 2018) using choice variables
712 which selected between 0 and 1. This approach was unable to find feasible solutions for inverse
713 photonics in less than 10 hours. For table sharding we obtained solutions by using a choice variable
714 for each table, selecting one of the available devices. This approach was not able to outperform the
715 greedy baseline and took longer time so it was strictly dominated by the greedy approach.

716 **Solution Prediction** We made several attempts at training solution predictors for each of our
717 domains. We label each problem instance with the best-known solution obtained (including those
718 obtained via SurCo). Note that predicting feasible solutions to combinatorial optimization problems
719 is nontrivial for general settings.

720 We evaluate solution prediction architectures in each setting. The models here match the architecture
721 of SurCo-prior but the output is fed through a sigmoid transformation to get predictions in $[0,1]$. In
722 nonlinear shortest path we use a GCN architecture and predict $[0,1]$ whether edges are in the shortest
723 s-t path. Not surprisingly, we found that predicting solutions to combinatorial problems is a nontrivial
724 problem, further motivating the use of SurCo which ensures combinatorial feasibility of the generated
725 solution.

726 Note that the solutions predicted by the networks may not be binary (and thus not feasible). We
727 then round the individual decision variables to get binary predictions. Empirically, we found that
728 our predictions are very close to binary, indicating that rounding is more a numerical exactness
729 operation than an algorithmic decision, with the largest distance from any original to rounded value
730 being 0.0008 for inverse photonics, 0.0001 for nonlinear shortest path, and 0.0007 for the assignment
731 problem of table sharding.

732 We evaluate the results on unseen test instances in Table 3 and find that these solution prediction
733 approaches don't yield combinatorially feasible solutions. We present machine learning performance
734 in the table below to verify that the predictive models perform "well" in terms of standard machine
735 learning evaluation even though they fail to generate feasible solutions.

736 We also iterate on table sharding to produce two more domain-specific approaches. We evaluate a
737 model variant which assigns each table into one of the 4 devices using softmax, which empirically
738 fails to yield feasible solutions that meet device memory limits for any of our instances. We further

Setting	Decision Variable Accuracy Average	Solution Accuracy	Solution Feasibility Rate
Inverse Photonics - Sigmoid	87%	0%	0%
Nonlinear Shortest Path - Sigmoid	95%	0%	0%
Table Sharding - Sigmoid	92%	0%	0%
Table Sharding - Softmax	88%	0%	0%
Table Sharding - Softmax + Iterative	70%	0%	100%

Table 3: Solution prediction results, most methods give infeasible solutions.

Setting	% Latency Increase vs Domain Heuristic (worst baseline)
DLRM-10	6%
DLRM-20	5%
DLRM-30	9%
DLRM-40	7%
DLRM-50	3%
DLRM-60	11%

Table 4: Comparison of only feasible solution prediction method against worst baseline.

739 develop a method called Softmax + Iterative which iteratively assigns the most likely table-device
740 assignment as long as the device has enough memory to hold the device. Luckily, this Softmax +
741 Iterative method empirically yields feasible solutions in this setting but we note that this approach is
742 not guaranteed to terminate in feasible solutions, unlike SurCo. To see why Softmax + Iterative does
743 not necessarily guarantee feasible termination, consider assigning 3 tables (2 small and 1 large) to 2
744 devices each with memory limit of 2, the small tables have memory 1 and the large table has memory
745 2. If the model’s highest assignment probability is on the small tables being evenly distributed across
746 devices, the algorithm will first assign the small tables to devices 1 and 2 but stall because it is unable
747 to assign the large table since neither device has enough remaining capacity. We present results for
748 this Softmax + Iterative approach compared to our domain heuristic which is the worst performing
749 baseline in Table 4.

750 For each setting, we evaluate the three metrics:

- 751 • **Decision Variable Accuracy Average**, is the average percent of variables which are correctly
752 predicted.
- 753 • **The solution accuracy**, is the rate of predicting the full solution correctly (all decision
754 variables predicted correctly).
- 755 • **The solution feasibility rate**, is the percent of instances for which the predicted solution
756 satisfies the constraints.